

Improved GIS Techniques and a Novel Physico-Chemical Risk Index for Surface Water Quality Assessment: A Case Study of the Al-Garraff Oil Field

Khaldoon T. Falih^{a,c}, Siti Fatin Mohd Razali^{a,b*} & Khairul Nizam Abdul Maulud^{a, b}

^aDepartment of Civil Engineering,

^bSmart and Sustainable Township Research Centre,

Faculty of Engineering & Built Environment, Universiti Kebangsaan Malaysia, Malaysia.

^cCivil Techniques Department, Nasiriyah Technical Institute, Southern Technical University, Iraq

*Corresponding author: fatinrazali@ukm.edu.my

Received 11 August 2024, Received in revised form 23 October 2024
 Accepted 23 November 2024, Available online 30 January 2025

ABSTRACT

Petroleum hydrocarbons and waste streams have polluted the environment, harmed human health, affected socio-economic conditions, and impacted communities in oil-producing countries. The aim of the study is to identify hotspots of contaminated water, create spatial risk maps of pollution from the petroleum industry and develop a novel index to estimate ecosystem pollution named physico-chemical risk index (PRI). Ten sites in the Al-Garraff oil field were analyzed for their water quality. The highest results of the six-month sample analysis were PH (8.7), DO (11.5 mg/L), turbidity (70.3 NTU), temperature (34 C), BOD₅ (37.8 mg/L), COD (101 mg/L) and TSS (109 mg/L). To achieve the above objectives, different methods and techniques were used; one of them is inverse distance weighting (IDW) with GIS to create geographical maps of the measured parameters. The IDW method was used to accurately map the distribution of ecosystem parameters of the oil field. The PRI was performed to compare the threshold values for pollutant elements with the contamination of the site. The threshold value for contaminated water in Garraf oil field is 24.328 and is determined by the PRI index. The analysis is carried out at regular intervals and compared with the threshold values. This work has created an important database for the oil industry that should be used to monitor ecosystems.

Keywords: geographic information system (GIS); inverse distance weighting (IDW); physico-chemical risk index (PRI); water contamination; oil field.

INTRODUCTION

The challenge of ensuring global access to clean water in the twenty-first century is enormous. Water resources, which are unevenly distributed across the Earth's surface, are deteriorating as a result of human activities (U.Farooq et al. 2015). Despite the increasing demand for water, efforts are being made to conserve water (Reza and Singh 2010; Okonofua, Lasisi, and Egbiki 2020).

Water pollution occurs when chemical, physical or biological elements cause a body of water to no longer be able to fulfill its intended function (Falih et al. 2024). The degree of pollution varies depending on the type, location, and use of the water body. In recent studies, researchers have focused on petroleum-related pollution and excluded

natural pollution (Schweitzer and Noblet 2018). Discharges of untreated water into rivers and urban runoffs have a negative impact on surface water quality and harm soil, groundwater, and the surrounding ecosystem. Understanding these impacts, as well as the characteristics of effluents, is essential for solving river pollution problems and understanding the spatial and temporal evolution of water quality. In many less developed countries, water quality assessment and sanitation infrastructure lag behind population and industrial growth (Ahmed et al. 2010).

Heavy metals (HM) pose a significant threat due to their persistence and toxicity in water (Proshad et al. 2021; Noraini Ruslan, Jannatulhawa Jasni 2021). Metals such as iron (Fe) and copper (Cu) are essential within certain limits, but exceeding these limits can be harmful. Other metals

such as cadmium (Cd), chromium (Cr) and cobalt (Co) are harmful even in trace amounts and can cause various health problems. For example, exposure to lead (Pb) causes memory loss and behavioral changes in children (Muhammad and Usman 2022; Abdul Maulud et al. 2021). The thermal properties of surface waters have a direct impact on aquatic life (Jurgelenaite, Kriaučiuniene, and Šarauskiene 2012). Variables such as temperature, dissolved oxygen and pH are influenced by factors such as weather conditions and geographical location (Ashkanani et al. 2019). The pH influences the solubility of metals and microbial activity. While rivers with humic substances can have an acidic character, petroleum residues can change the pH (Gandaseca et al. 2011; Mhamdi, Khouni, and Ghrabi 2016). Total suspended solids (TSS), chemical oxygen demand (COD) and biochemical oxygen demand (BOD₅) are indicators of water quality and reflect the presence of pollutants and organic matter (Bilotta and Brazier 2008; Khan, Gani, and Chakrapani 2016; Wan Mohtar et al. 2019). By measuring the ambient concentrations and comparing the maximum values with the parameters, it is possible to determine whether certain parameters exceed the optimal values or are approaching harmful thresholds that affect the habitat and growth of aquatic life (Nguyen, Diem, and Huynh 2023; Nguyen and Truong 2023)

Turbidity, which is influenced by particles and biological activity, affects the translucency of water (Putnam and Pope 2003). Dissolved oxygen (DO) varies with temperature, salinity, and water flow. Stagnant water contains less oxygen than flowing water, and cold, fresh water has a higher oxygen binding capacity than warm, salty water. Geographic information systems (GIS) are invaluable tools for a holistic assessment of water quality because they seamlessly integrate spatial and temporal variations (Mtetwa, Kusangaya, and Schutte 2003; Li and Heap 2011). This technology helps visualize complex relationships and provides scientists and resource managers with a robust platform for analysis and simulation (Arslan 2001; Oke and Ogedengbe 2013). GIS has evolved beyond mere software for managing and processing geographic information. It now encompasses the management and processing of all types of geographic information ((Panigrahy 2021; Chen et al. 2024). Geographic information systems (GIS) are proving to be invaluable tools for holistic water quality assessment as they seamlessly integrate spatial and temporal variations (Dongquan et al. 2009; Syed Abdul Rahman et al. 2022).

Water quality monitoring is of paramount importance to guide action against water pollution and ensure proper implementation of prevention and intervention programs (Zaiedy, A. Karim, and Abd Mutalib 2016; Ata et al. 2018). A comprehensive assessment of water quality is beneficial

for evidence-based management and conservation of water resources, for the development and implementation of water treatment and sanitation systems that ensure the safety of water used in agriculture, and for the adoption and implementation of consumer and environmental laws and regulations (Mohd Soukhri et al. 2022). The assessment of water quality using environmental parameters involves several methods, including data analysis, modeling techniques, statistics, and water quality index (WQI) methodology (Singh, Majumder, and Vidyarthi 2023).

When selecting appropriate interpolation models, consistency with the research objectives and the specific characteristics of the study objects is of paramount importance (Qiao et al. 2018). However, the evidence for the superiority of one interpolation technique over another is inconclusive (Gong, Mattevada, and O'Bryant 2014). Consequently, kriging and inverse distance weighting (IDW) are two interpolation approaches that have been used extensively in pollution mapping and water assessment (Mirzaei and Sakizadeh 2016). Pankalagr and Jarag (2016) claim that the IDW method outperforms the kriging method in terms of accuracy, a position supported by El-Zeiny and Elbeih (2019). In addition, the study by Gong, Mattevada, and O'Bryant (2014) emphasizes that the IDW method provides excellent results in predicting concentrations of certain pollutants in water bodies and outperforms kriging in terms of accuracy.

To assess the utility and accuracy of the geochemical indexing methods used by various researchers in the past, a brief overview is required. A major limitation of conventional indices is that they cannot account for all components in a single calculation (Mohamad Hamzah et al. 2022). The aim of this study is to develop a new type of index for estimating the pollution of ecosystems, the so-called physico-chemical risk index (PRI). The PRI is derived from a mathematical formula that combines different environmental parameters into a single value, allowing a comprehensive assessment of environmental quality and suitability for different water use applications, with a weighting value for each pollutant.

The specific objectives of this research are: (i) to assess the feasibility of developing an approach to pollution assessment using a limited number of monitoring stations over a period of time, focusing on global advances that emphasize efficiency and cost-effectiveness without compromising accuracy; (ii) create a new index encompassing all measured physico-chemical elements and produce a corresponding map depicting pollution levels; (iii) visualize the spatial and temporal variations of these parameters using GIS-based interpolation and overlay analysis tools; and (iv) identify the areas most affected by petroleum activities and requiring urgent attention. In addition, this study demonstrates the accuracy of the IDW

method even with a limited sample size, which is a major challenge for environmental protection agencies that usually require numerous samples and longer time periods.

METHODOLOGY

The methodology of this study involved collecting samples from designated sites located in proximity to oil operations and subsequently determining the concentrations over six months. The primary parameters tested were temperature, pH, turbidity (TUR), COD, BOD₅, TSS, dissolved oxygen, and oil and grease. Thereafter, the water quality assessment was divided into two portions to ascertain the level of

contamination in the study area. The initial step is to employ geographic information systems methodologies to provide a comprehensive understanding of the concentrations of these elements at every location inside the oil field.

These methodologies enable the forecast of all locations by utilizing the data collected from the measured stations. The second phase involves creating a novel index to quantify pollution by utilizing the most extensive set of components and assigning weight (indicating the impact on pollution levels). Subsequently, the threshold limit for the research area will be determined, and the monthly findings will be compared with the acceptable pollution standard. As shown in Figure 1.

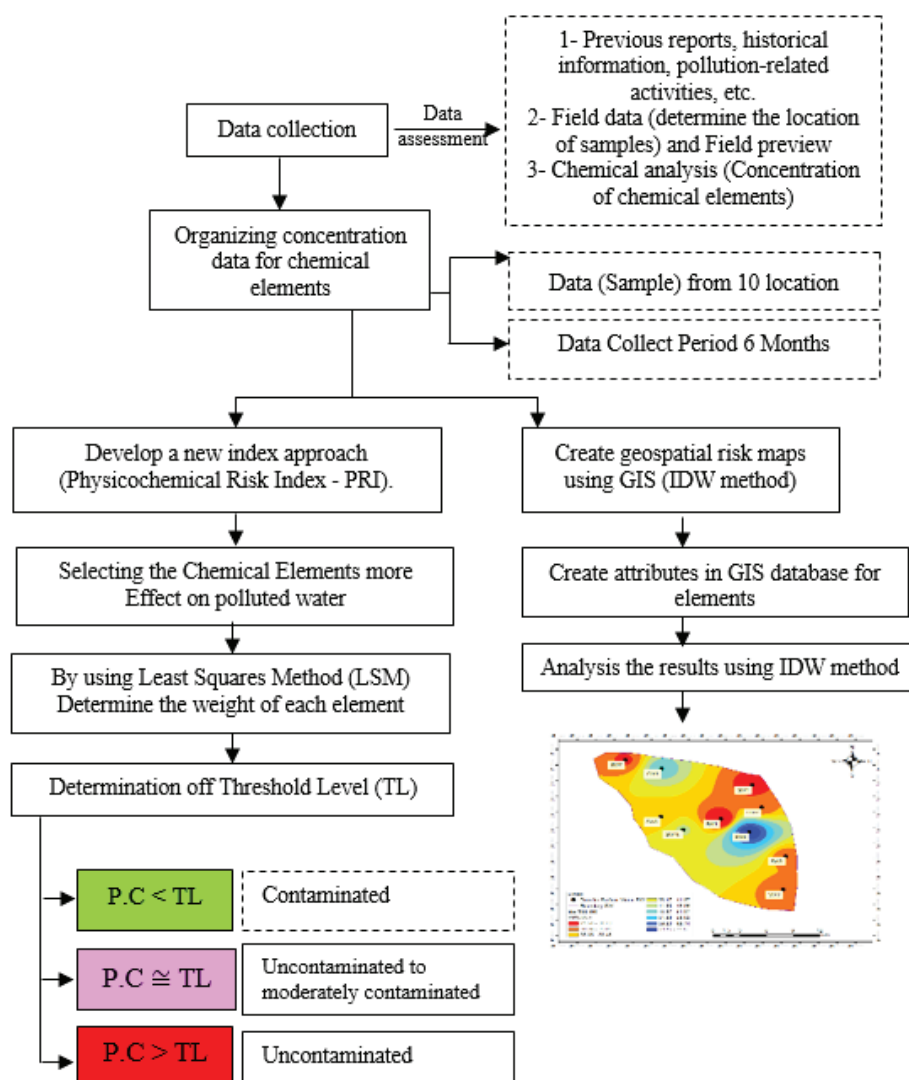


FIGURE 1. Flowchart of research methodology.

WATER SAMPLING

Water quality is the first critical factor to evaluate when determining the extent of pollution and selecting the best available solutions. This value can be influenced by numerous factors such as geological location, weather, human activities, or site conditions. While it is relatively simple to identify, understand and manage pollution sources such as domestic or industrial wastewater, it becomes more complicated when it comes to pollution of areas such as rural or agricultural land (Haldar et al. 2020).

This study focuses on the Garraf oil field in southern Iraq, located between 31° 38' 15" to 31° 40' 53" N and 45°

51' 20" to 46° 2' 54" E. To comprehensively monitor water quality in secondary streams flowing through or near the oil field and discharging into numerous agricultural and residential areas, multiple samples were collected from March to August 2022. Samples were collected at ten locations along the streams to assess the level of pollution and to examine the physical and chemical characteristics of the streams in the area (see Figure 2). Sampling sites were selected based on potential sources of pollution, focusing on areas near oil field facilities as well as residential and agricultural areas surrounding the field. The coordinates of the sampling sites in latitude and longitude are listed in Table 1.

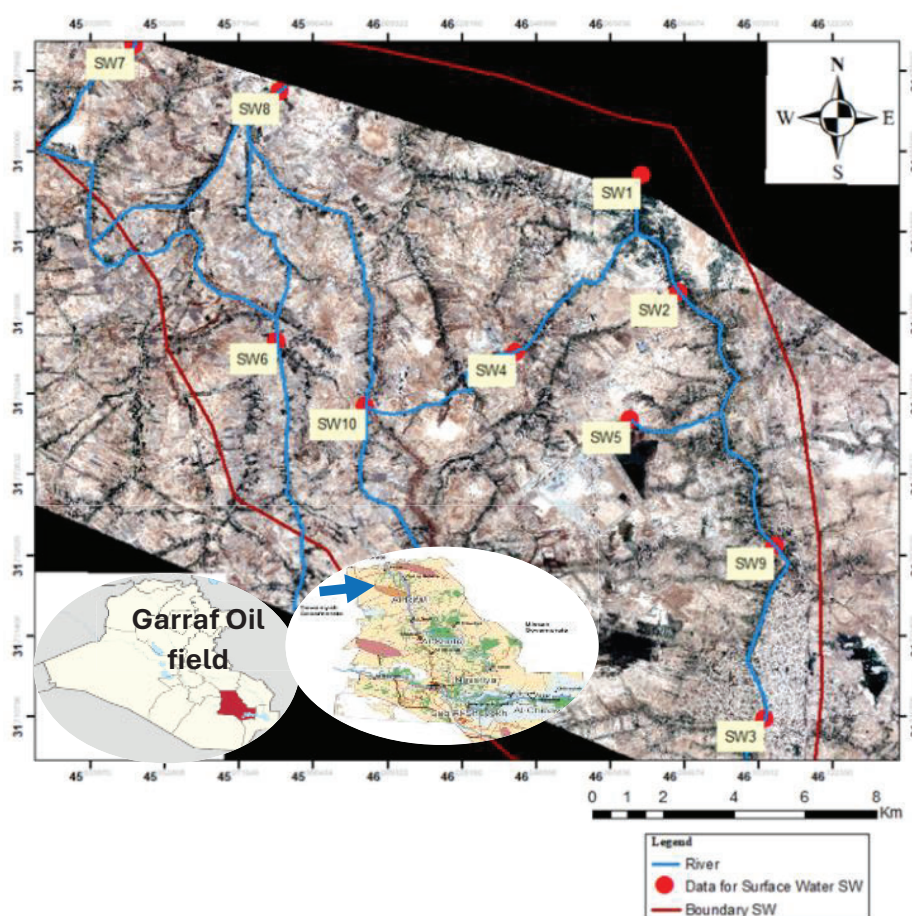


FIGURE 2. Geographical location and distribution of sampling sites in the Gharraf oil field.

WATER QUALITY ASSESSMENT

The Water Quality Assessment (WQA) serves as a comprehensive database of water quality indicators for the region’s sub-stream systems. During the six-month study period (March to August 2022), we monitored physical and chemical parameters to gain a baseline understanding

of water quality in these rivers. This article focuses primarily on the most important parameters, including temperature (measured in the field with a thermometer and analyzed according to the ASTM E-2877 method), pH (measured with a Consort C860 pH meter), and TSS, which was determined by filtering the samples with 0.45 m filter paper according to (Bukhari 2008; Zaiedy, A. Karim, and

Abd Mutalib 2016). In addition, elements such as dissolved oxygen (DO) (measured using a dissolved oxygen meter), turbidity (measured using a turbidity meter), biochemical oxygen demand (BOD5) (measured using a BOD meter), chemical oxygen demand (measured using a COD meter), oil and grease were also assessed.

TABLE 1. Identification of the sampling stations with their respective geo-coordinates along the surface water in the Garraf oil field.

Station	Location	Longitude	Latitude
SW1	GR	31° 50' 56.74" N	46° 04' 25.31" E
SW2	GR	31° 49' 09.20" N	46° 04' 59.40" E
SW3	GR	31° 42' 37.38" N	46° 06' 18.48" E
SW4	TGR	31° 48' 13.83" N	46° 02' 30.84" E
SW5	GL	31° 47' 11.94" N	46° 04' 15.65" E
SW6	TGR	31° 48' 24.28" N	45° 58' 52.80" E
SW7	TGR	31° 54' 7.29 " N	45° 58' 20.95" E
SW8	TGR	31° 52' 46.19 " N	45° 59' 13.42" E
SW9	GR	31° 45' 16.24" N	46° 06' 27.88" E
SW10	TGR	31° 47' 24.25" N	46° 00' 13.74" E

*GR: Garraf River, TGR: Tributary of Garraf River; GL: Garraf Lake

GIS-BASED ASSESSMENT OF WATER QUALITY

ArcGIS, developed by ESRI, played a vital role in data input, analysis and mapping. The base map with the boundaries of the Garraf oil field was provided by the Thi-Qar Oil Company (TOC). The raster data of the base map was converted into vector data and the coordinates of the sampling points were recorded using GPS. ArcCatalog was used to create the database of water quality indicators and the river network, while ArcGIS 10.7 extensions facilitated analysis, interpolation, and mapping.

For the inverse distance weighting (IDW) method, which was implemented with the Spatial Analyst extension in ArcGIS 10.3, the results of laboratory tests at ten distinct locations along the rivers were used. The additional data collected for each parameter at the measurement points was used to calculate the interpolated cells for the creation of the river basin maps.

GIS INTERPOLATION WITH INVERSE DISTANCE WEIGHTING (IDW)

For spatial interpolation, inverse distance weighting (IDW) was used, which is accessible via the Geostatistical Analyst toolbar in ArcGIS. IDW is a widely used method for mapping variables that is known for its accuracy and convex interpolation. It is suitable for continuous models of spatial variation and has its roots in mining and geological engineering, where it is based on distance-weighted locations (Jones, Davis, and Sabbah 2003; Alssgeer et al. 2018). The IDW method within the GIS program has made a name for itself.

For its accuracy in delineating pollution zones and identifying spatial patterns. It emphasizes the validation of results through a limited sample size and takes into account several factors that influence the observed physical and chemical characteristics. Equation (1) is the equation used for IDW.

$$Z(X_0) = \frac{\sum_{i=1}^n z(x_i) \cdot d_{ij}^{-p}}{\sum_{i=1}^n d_{ij}^{-p}} \quad (1)$$

where Z is the value interpolated for a grid node; Z_i represents adjacent data points; and d_{ij} measures the distances between each grid node and the data point.

EVALUATION OF ACCURACY

To evaluate the accuracy of the interpolation technique, validation experiments were performed using an iterative jackknife method. In this method, interpolation is performed iteratively for all data points, excluding each point in turn. The resulting interpolated values are the calculated values, which were compared with the observed values using a cross-validation statistic to summarize the differences (Wilk et al. 2006). The process is repeated n times, where n is the total number of samples, and the calculated statistics are used as a diagnostic to determine the feasibility and suitability of the interpolation method for risk maps generation (Khouni, Louhichi, and Ghrabi 2021; Simpson and Wu 2014). Cross-validation tests integrated into the output of the Geostatistical Analyst Toolbar in ArcGIS 10.7.1 provide exploratory analysis results (Wu et al. 2019).

The ME and RMSE, for example, are two cross-validation statistics that explain the differences between observed and estimated values. ME provides a displacement prediction of the error sequence and an absolute measure of the magnitude of the error, while RMSE indicates the

accuracy of spatial analysis in geographic information systems and reflects the sensitivity as well as the extreme predicted values (Njeban 2018).

To estimate interpolation accuracy, we also evaluate R^2 , which is commonly used to measure the correlation between predicted and measured values. The formulas for ME, RMSE, and R^2 are as follows:

$$ME = \frac{1}{N} \sum_{i=1}^N (\hat{Z}(X_i) - Z(X_i)) \tag{2}$$

$$RMSE = \sqrt{\frac{1}{N} \sum_{i=1}^N (\hat{Z}(X_i) - Z(X_i))^2} \tag{3}$$

where $\hat{Z}(X_i)$ is the predicted value and $Z(X_i)$ is the observed value.

$$R^2 = \frac{[\sum_{i=1}^N (P_i - P_{avg}) \sum_{i=1}^N (O_i - O_{avg})]^2}{\sum_{i=1}^N (P_i - P_{avg})^2 \sum_{i=1}^N (O_i - O_{avg})^2} \tag{4}$$

where P_{avg} is the mean estimated value and O_{avg} is the mean observed value. O_i is the observed value, while P_i is the predicted value. N is the number of samples, while n is the number of estimated values.

RESULTS AND DISCUSSION

This section presents and discusses the results of the sample concentrations of the elements that were determined in the laboratories and subsequently presented in tabular form to prepare them for data analysis. The spatial analysis of the

distribution of pollutants in the study area is conducted using maps, as described in the methodology of the study. The distribution method is also explained. The degree of pollution is then determined using a globally recognized index. Finally, the methodology and procedure for creating a new index are presented and this index is compared with other commonly used indices.

To determine the spatial arrangement of the hazardous and polluted zones, we performed a multi-site analysis within and near the hydrocarbon field using inverse distance weighting (IDW) predictions. This approach helps to quantify pollution risks at different river sites and enables the identification of priority intervention zones and the determination of eligibility (Yan et al. 2015). Spatial interpolation of risks using GIS and IDW techniques is a valuable tool for assessing surface water quality, as other researchers have shown (Oke and Ogedengbe 2013; Dheenan et al. 2014)

MONITORING AND SPATIAL INTERPOLATION OF PHYSICO-CHEMICAL PARAMETERS

The management of surface waters requires careful analysis of parameters such as pH, dissolved oxygen (DO), turbidity (TUR), temperature, biochemical oxygen demand (BOD5), chemical oxygen demand (COD), TSS, oils and fats. The comprehensive physico-chemical analysis of the water samples from the Garraf oil field is shown in Table 2. With the help of GIS and IDW interpolation techniques, the spatial maps were able to clearly show the progressive behavior of the physico-chemical pollutants identified. The gradual fluctuations of the pollutant levels along the Garraf oil field are obvious. The interpolation technique using the blue color for pollutants and the red color for safe zones visually highlights the variations in water purity throughout the Garraf oil field.

TABLE 2. Summary of the mean values of the physico-chemical parameters of the surface water samples from the Garraf oil field.

Parameter	Unit	Sample ID/ Category										Analysis Apparatus	Analysis Method	Max. allowable Iraqi National limits
		SW1	SW2	SW3	SW4	SW5	SW6	SW7	SW8	SW9	SW10			
PH	-	7.4	8	7.8	8	7.7	8.5	8.7	8.7	7.8	8.1	pH meter	ASTM D-1293	6.5 -8.5
DO	mg/L	11.5	11.5	9.8	6.5	11	9.1	8.9	10.8	11	9.3	DO meter	ASTM D-888	> 5
TUR	NTU	44	53	61	12	59	12	70.3	60	68	33	Turbidity meter	ASTM D-1889	50 NTU
Temp.	°C	32	29	31	28	28	28	33	31	34	30	Thermometer	ASTM E-2877	-

continue ...

... cont.

BOD ₅	mg/L	19.9	21.2	21.9	19.8	37.8	24.2	23.5	27	20.2	27	BOD meter	APHA 5210-B	30
COD	mg/L	31	35	37	32	101	43	43	72	38	66	COD meter	ASTM D1252	100
TSS	mg/L	36	37	45	30	109	43	37	61	36	52	Gravimetric	ASTM D-5907	100
Oil & grease	mg/L	1.15	1.35	1.63	0.85	2.80	2.67	2.98	2.98	3.03	1.48	Oil in water meter	ASTM D-3921	10
E. Coli	-											Growth Culture	HIMEDIA M1713	

TOTAL SUSPENDED SOLID (TSS)

The total suspended solids (TSS) concentrations measured during our surveys show a natural variation from 22 mg/L at station SW4 to 80 mg/L at station SW5, with all values below the highest Iraqi standard value of 100 mg/L. Elevated concentrations of suspended solids are often the result of human activities as well as urban and industrial discharges, as observed in our study, where the highest TSS levels are likely due to industrial processes related to petroleum production. Such elevated TSS levels can have a negative impact on water quality as they affect turbidity, light transmission and the photosynthetic process (Bilotta and Brazier 2008).

The spatial distribution of TSS shown in Figure 3 indicates that Garraf Lake, located in the project area near the Garraf Base Camp, has significantly higher

concentrations of suspended solids compared to other areas, with predicted TSS concentrations ranging from 73 mg/L to 79 mg/L. These trends are associated with wastewater from the petroleum industry. In particular, the region with the highest concentration of soluble solids (SW5), shown in blue, is associated with the discharge of petroleum processing fluids.

The slight decrease in TSS concentration in the Garraf tributary downstream of the landfill area (SW6), followed by an increase with increasing flow in both areas (SW8-SW10), could be the result of increased suspended solids concentrations caused by municipal, industrial and agricultural runoff in the regions area, with predicted TSS concentrations ranging from 73 mg/L to 79 mg/L. These trends are associated with petroleum industry effluents. In particular, the region with the highest concentration of soluble solids (SW5), shown in blue, is associated with the discharge of petroleum processing fluids.

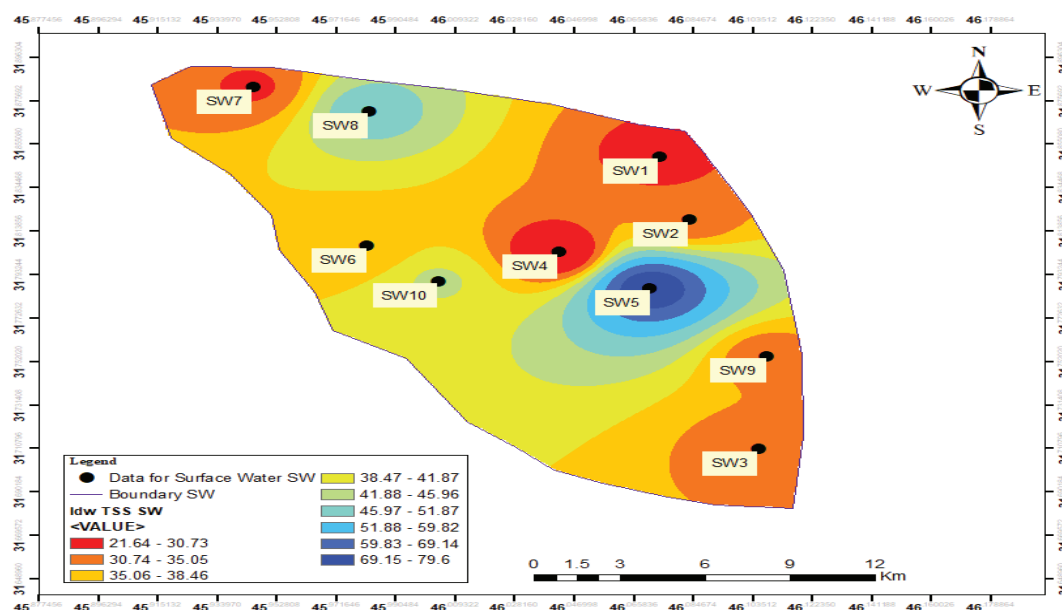


FIGURE 3. Spatial distribution of total suspended solids (TSS) in mg/L in the Garraf oil field.

CHEMICAL OXYGEN DEMAND (COD)

In this study, COD concentrations (Figure 4) were highest at sampling site SW5 (Garraf Lake – within the project area near the Garraf base camp) with a mean value of 80 mg/L, while sampling site SW1 (Garraf River – upstream of the project area) had the lowest COD concentration with a mean value of 20 mg/L. Importantly, the COD concentrations at all river sites were below the Iraqi limit of 100 mg/L.

The IDW interpolation map shown in Figure 4 predicts COD concentrations between 19 mg/L and 79 mg/L, all of which are below the 100 mg/L limit set by Iraqi regulations. However, upon closer inspection of the sampled regions, the blue colored areas, particularly SW5, showed the highest concentrations in the range of 73-79 mg/L, indicating proximity to petroleum operations. In contrast, the dark red colored areas (SW1, SW2 and SW4) showed lower concentrations, ranging from 19 to 26 mg/L.

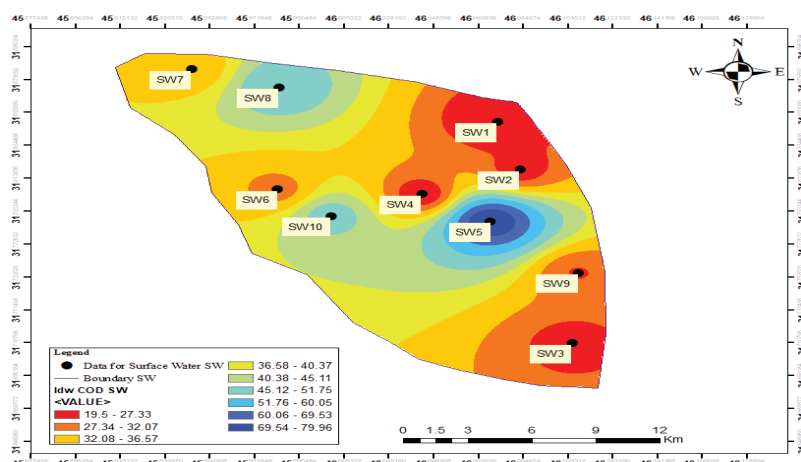


FIGURE 4. Spatial distribution of chemical oxygen demand (COD) in mg/ L in the Garraf oil field.

BIOCHEMICAL OXYGEN DEMAND (BOD₅)

The spatial interpolation of the BOD₅ showed the distribution of the organic load of the surface water and the influence of the oil from the al-Garraf oil field on the

discharge (see Figure 5). The coherence between the BOD₅ and COD distribution could be due to the correlation between these two pollutant indicators. In particular, the industrial areas along the river system had the highest BOD₅ values, with predicted concentrations ranging from 27 to 29 mg/L.

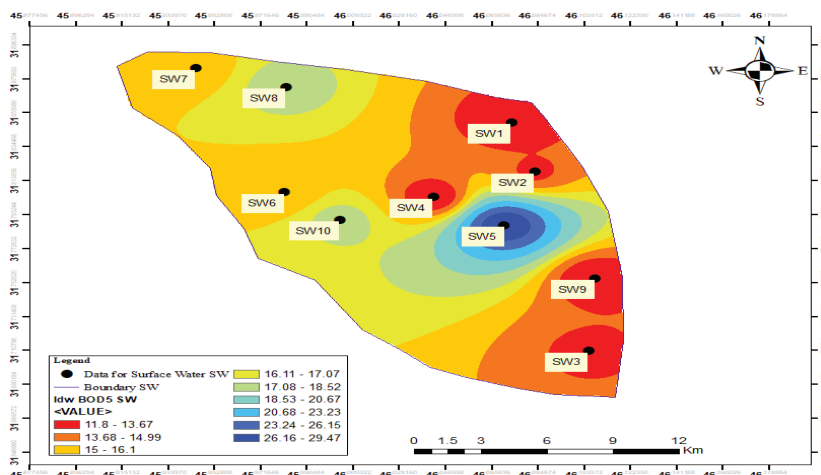


FIGURE 5. Spatial distribution of biochemical oxygen demand (BOD) in mg/ L in the Garraf oil field

Downstream of the project site (SW8) on the Garraf tributary, a conspicuous orange-yellow coloration indicated moderate pollution, with organic matter concentrations ranging from 17 mg/L to 19 mg/L. The BOD5 content of the Garraf River decreased significantly upstream of the project site, and this trend continued in the Garraf tributary downstream of the landfill.

contrast, sampling site SW4, a tributary of the Garraf upstream of the Garraf base camp, had the lowest turbidity concentration with an average of 8 mg/L. It is noteworthy that many tributaries exceeded the Iraqi standards and reached turbidity values above the limit of 100 mg/L.

DISSOLVED OXYGEN (DO) AND TURBIDITY (TUR)

In our study, sampling site SW7, a tributary of the Garraf River downstream of the project site, had the highest turbidity concentration with an average of 55 mg/L. In

Looking at the interpolation map of turbidity values in Figures 6, the strikingly high turbidity and freshness values at sampling point SW9 stand out. At this point, which is located downstream of GA4 on the Garraf, concentrations between 50 and 55 NTU were measured near the end of our surface water sampling line. This increase in turbidity is attributed to suspended solids and chemicals from petroleum processing. It is also worth noting that the vast majority of our samples exceeded the Iraqi standard of 50 NTU.

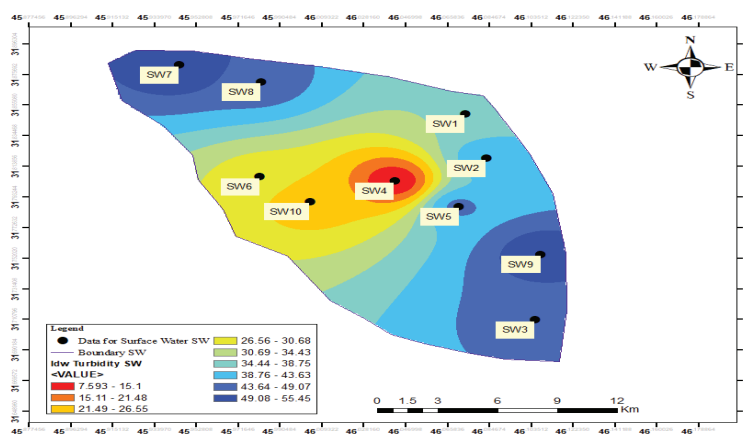


FIGURE 6. Spatial distribution of turbidity in NTU in the Garraf oil field.

The spatial interpolation of dissolved oxygen in Figure 7 shows that the values are acceptable and meet the required

values, which should be above 5 mg/L according to Iraqi standards.

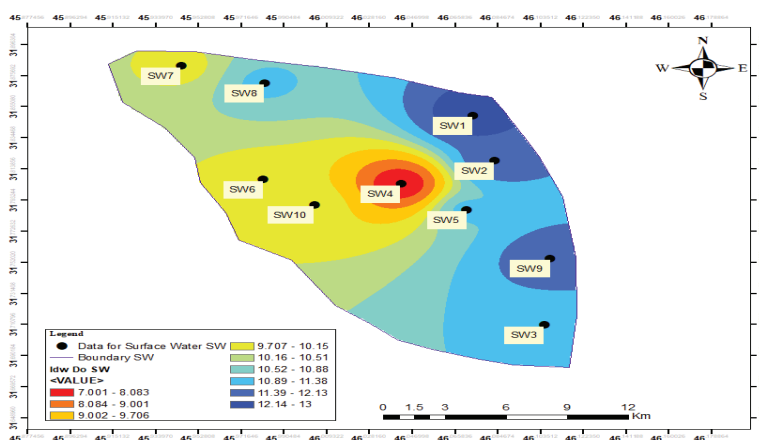


FIGURE 7. Spatial distribution of dissolved oxygen (DO) in mg/L in the Garraf oil field

ACCURACY ASSESSMENT AND CROSS-VALIDATION OF IDW

All researchers dealing with interpolation agree that the goal is the guaranteed accuracy of data inserted between points with known values. The bias of the spatial interpolation algorithm is directly proportional to the proximity of its underestimation to the corresponding real observations, which affects its accuracy (Sekulić et al. 2020). In our study of surface water quality assessment in the Garraf oil field, we examined the accuracy of the IDW interpolation method using three key statistical criteria: RMSE, ME and R^2 .

In validating the model, we used the participating variables with the smallest RMSE and ME, both approaching 0, and the highest values for R^2 , approaching 1 (Njeban 2018). Table 3 describes the RMSE, ME and R^2 parameters for each physico-chemical characteristic investigated to provide a common overview for further consideration. The predictive accuracy of the inverse distance weighting (IDW) method for water quality in the Al Garraf oil field shows through cross-validation that it has a high level of prediction for each of the parameters studied.

Cross-validation yielded mean error (ME) values close to zero, which underlines the accurate reproduction of the spatial distribution by the theoretical models and shows a strong correlation with the spatial patterns (see Table 3). However, caution should be exercised when interpreting the ME, as positive and negative estimates cancel each other out, resulting in an underestimated measure of true error (Ikechukwu et al. 2017). Therefore, the RMSE was used as it measures sensitivity to outliers and reflects the magnitude of the extreme error.

TABLE 3. Cross-validation results for the IDW interpolation method used to assess surface water quality in the Al-Garraf oil field.

Criteria	ME	RMSE	R^2
TSS	0.00503	0.27560	0.988
COD	0.00528	0.30676	0.989
BOD5	0.00111	0.08489	0.989
Turbidity	-0.0032	0.20815	0.995
DO	0.00024	0.02128	0.995

The relatively low and comparable RMSE values for all physico-chemical parameters, ranging from 0.005 for pH to almost 0.30676 for COD, confirm the validity of the pronounced central trends and minimal extreme error (Yavuz and Erdoğan 2012). In our study, R^2 reached remarkably high values, ranging from 0.988 for TSS, to 0.996 for pH in the surface water of the Garraf oil field.

These high R^2 values indicate robust agreement between observed and IDW-interpolated values.

The spatial distribution maps showed the intensity distribution of the measured elements for all stations in the oil field as determined by analyzing the data with (GIS) techniques (IDW method). It was found that continuous monitoring of the high intensity stations is required. For example, turbidity should not exceed 50, but at stations SW2, SW3, SW5, SW7, SW8 and SW9 this limit was exceeded. This indicates that the waste is not being filtered sufficiently and is entering the water directly.

The permissible limit value for the element (BOD) was exceeded at the station (SW5) and is approaching the limit value at several other stations. This substance has a significant impact on the mortality of aquatic organisms. The same applies to the element (COD), which has a significant impact on aquatic life and exceeds the permitted limit for the same station. Suspended solids also exceed the permitted limit at this station. This element has a significant impact on the purity of the water, especially the water used for agricultural irrigation.

INDICES FOR ASSESSING POLLUTION IN SURFACE WATER

POLLUTION DEGREE INDEX (PDI)

The assessment of surface water pollution by measuring concentrations of chemical and physical parameters is limited to a handful of mathematical methods and indicators, with the exception of the Pollution Degree Index (PDI) and some other indices. Metal pollution in water is assessed using the Metal Index parameter (Anjum, 2019). The index quantifies the concentration of pollutants in water compared to the maximum concentrations set by regulatory agencies such as the Environmental Protection Agency (EPA) and the World Health Organization (WHO) (Ramal, Jalal, and Abdulhameed 2021). The metal index provides important insights into the safety and overall quality of water. The calculation is based on the following formula:

$$PDI = \frac{C_s}{C_m} \quad (5)$$

where C_s is the metal concentration in a sample and C_m is the maximum allowed concentration.

The pollution index was calculated to assess the metal pollution of the surface water in the Garraf oil field (see Table 4) using Equation 5. The pollution index values for dissolved oxygen (DO), turbidity (TUR), biochemical

oxygen demand (BOD), chemical oxygen demand (COD), total suspended solids (TSS) and oil and grease were calculated and presented graphically in Figure 8.

The metal index values showed a decreasing order, with $DO > Tur > BOD > TSS > COD > oil$. In general, the metal index values for all parameters were below 1, except for oil, where the value was above 1. This index indicates

that the surface water in the Garraf oil field is only slightly contaminated. The presence of this indicator is an indication of the safety and long-term viability of the water in this region (Goher et al. 2014). Nevertheless, continuous monitoring of these metals is essential to ensure compliance with acceptable limits in the long term.

TABLE 4. Pollution index in the surface water of the Garraf oil field

Parameter of analysis	C_s	C_m	PDI
DO (mg/L)	10.86	>5	2.17
TUR(NTU)	15.74	16.66	0.9447
BOD (mg/L)	15.8	30	0.5266
COD (mg/L)	36.2	100	0.362
TSS (mg/L)	38	100	0.38
Oil & Grease (mg/L)	2.09	10	0.209

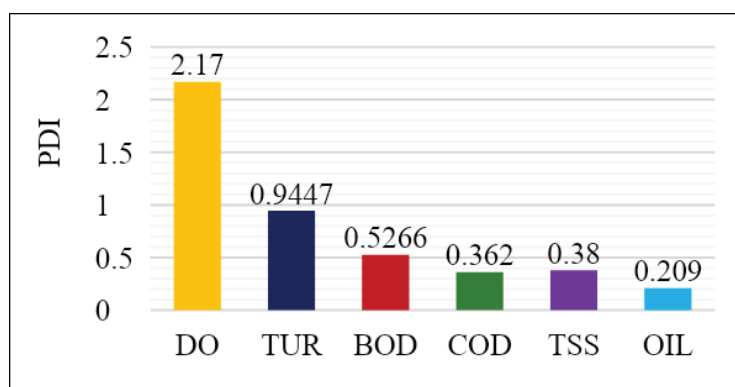


FIGURE 8. Calculated pollution degree index values for DO, TUR, BOD, COD, TSS, and Oil & grease.

NOVEL INDEX: PHYSICO-CHEMICAL RISK INDEX (PRI)

This study presents a robust methodology that focuses on the assessment of trace element concentrations in a potentially contaminated area and compares them to the limits set by Iraqi standards. A unique mathematical equation is then developed to assess contamination at specific sites, called the physico-chemical risk index (PRI), which weighs the different components and applies the least squares method. A comparative analysis is then conducted to assess the correlation between the element thresholds and the measured contamination levels at the site in question.

The determination of the threshold for a particular site is of paramount importance and serves as a safety threshold that sets the upper limit for the concentration of a particular element above which no adverse effects are expected. This is in line with the regional geochemical baseline. The

threshold for mandatory investigations defines the concentration of an element at which potentially hazardous effects are to be expected (Frutos et al. 2010). The threshold thus represents the numerical value at which a particular site is considered potentially contaminated.

The focus is on selecting the physico-chemical elements with the strongest effects. It is therefore important to identify the components that have the greatest impact on water pollution. Therefore, the elements DO, Tur, BOD, TSS, COD as well as oils and grease were selected for further analysis. The mass of each element used in the equation is determined, with each element considered as an individual unit. The theory or methodology of least squares is considered one of the most important approaches for determining the weight. After determining the weighting and considering the maximum allowable values of the elements, the threshold value is determined to classify the site as contaminated or uncontaminated.

FRAMEWORK OF PHYSICO-CHEMICAL RISK INDEX (PRI)

In order to develop a novel index tailored to each scenario, a basic framework must be created to facilitate the systematic collection and organization of relevant data. In this study, the model of primary petroleum contamination by PRI detection was formulated using equation (6), in which selected measured heavy elements were included. The inclusion of these elements allows for the potential selection of additional elements for future research using the same methodology.

$$\text{PRI} = \text{DO} (W_{\text{DO}}) + \text{TUR} (W_{\text{TU}}) + \text{BOD} (W_{\text{BOD}}) + \text{COD} (W_{\text{COD}}) + \text{TSS} (W_{\text{TSS}}) + \text{Oil} (W_{\text{Oil}}) \quad (6)$$

where W is the weighting of the chemical elements and PRI is the physico-chemical risk index in the field.

Determining the weighting for each element, as given in equation (6), is critical due to the inherent variability of the effects of the different constituents on contamination. The least squares method was used to calculate the weighting according to equations (7) to (10). The weighting obtained can be used directly to assess the degree of contamination of a site by classifying it as contaminated or uncontaminated.

$$\bar{X} = \frac{\sum X}{n} \quad (7)$$

where X is the observed value and n is the number of measurements.

The residual is the discrepancy between the observed value and the estimated value of the variable of interest, e.g., the average of the values of a sample. In regression analysis, where these concepts are sometimes referred to as regression error and residuals, leading to the term sample residuals, the distinction is particularly noteworthy (Das 2019). Equation (8) defines the determination of residual errors, V .

$$V = X - \bar{X} \quad (8)$$

The term “variance” in equation (9) is a statistical metric that measures the extent of dispersion of values within a given data set. More specifically, variance (δ^2) measures the extent to which each value in the data set deviates from the mean, reflecting its importance in constructing the ideal model for determining pollution levels.

$$\delta^2 = \frac{\sum V^2}{n-1} \quad (9)$$

Some measurements have a higher precision due to several factors, such as the location of the sample, the effects of elements and the circumstances of the measurement. Therefore, it is important to apply relative weighting when adjusting measurements to obtain the best value for the measured variable. Equation (10) is used to calculate the weighting of the variables.

$$W = \frac{1}{\delta^2} \quad (10)$$

RESULT OF THE PHYSICO-CHEMICAL RISK INDEX (PRI)

This novel PRI index aims to measure pollutant concentrations directly and to ensure independence from intermediates that could affect the accuracy of the results.

As explained previously, to develop a new index for the assessment of contaminated elements, equation (7) is used to calculate the sum of the data values, which then leads to the determination of the mean value of the data set, as shown in Table 5. It shows the concentrations of the six-month samples for each element, including dissolved oxygen (DO), turbidity (TUR), biochemical oxygen demand (BOD), chemical oxygen demand (COD), total suspended solids (TSS), and oils and greases. The average concentrations are calculated in order to obtain a comprehensive overview of the data.

TABLE 5. Mean concentrations were recorded throughout 6 months.

Month	Concentration					
	DO (mg/L)	TUR (NTU)	BOD (mg/L)	COD (mg/L)	TSS (mg/L)	OIL (mg/L)
March	9.96	2.94	10.15	25.8	17.91	1.130
April	11.25	14.45	8.42	28.6	36.00	1.408
May	12.40	14.94	13.72	33.0	38.40	1.932
June	11.50	13.73	16.52	37.7	40.60	2.190

continue ...

... cont.

July	10.08	15.39	21.72	42.1	47.80	2.620
August	9.94	15.75	24.25	49.8	47.80	3.275
Total	65.13	77.20	94.78	217.0	228.51	12.555
Mean	10.86	12.87	15.80	36.17	38.09	2.0925

Equation (8) is then applied to determine the residual errors (V), as shown in Table 6. The residual errors represent the differences between the individual data points and the mean for each element. The variance (δ^2) is then

calculated using equation (9), resulting in Table 7. This table shows the variance for each element and provides information about the dispersion of the data points around the mean.

TABLE 6. Residual errors (V) for each element.

Residual Errors (V)					
DO	TUR	BOD	COD	TSS	Oil & Grease
-0.895	-9.923	-5.646	-10.366	-20.175	-0.962
0.395	1.585	-7.376	-7.566	-2.085	-0.684
1.545	2.076	-2.076	-3.166	0.315	-0.160
0.645	0.863	0.723	1.533	2.515	0.097
-0.775	2.520	5.923	5.933	9.715	0.527
-0.915	2.876	8.453	13.633	9.715	1.182

TABLE 7. Variance (δ^2) for each element.

Months	W_{DO}	W_{TUR}	W_{BOD}	W_{COD}	W_{TSS}	W_{Oil}
March	0.801	98.467	31.884	107.467	407.030	0.926
April	0.156	2.513	54.415	57.254	4.347	0.468
May	2.387	4.313	4.312	10.027	0.099	0.025
June	0.416	0.745	0.523	2.351	6.325	0.009
July	0.600	6.351	35.085	35.204	94.381	0.278
Aug.	0.837	8.276	71.458	185.867	94.381	1.398
$\sum V^2$	5.197	120.668	197.68	398.173	606.564	3.106
δ^2	1.039	24.133	39.536	79.634	121.312	0.621

Table 8 shows the weighting of the individual elements, bearing in mind that each element should be

treated differently in the evaluation process. The weights are determined on the basis of the previously calculated variance values.

TABLE 8. Weighting (W) for each element.

W_{DO}	W_{TUR}	W_{BOD}	W_{COD}	W_{TSS}	W_{Oil}
0.961	0.041	0.025	0.012	0.008	1.609

The Table 9 lists the maximum permissible limits for the individual elements in accordance with the Iraqi standards. These permissible limit values serve as the basis

for determining the total limit value according to equation (7), taking into account the weighting of the individual elements (Table 8).

TABLE 9. Maximum permissible limit for each element in the Iraqi standards.

Element	Max. Allowable in Iraqi standard
DO (mg/L)	5
TUR (NTU)	16.66
BOD (mg/L)	30
TSS (mg/L)	100
COD (mg/L)	100
OIL (mg/L)	10

Applying equation (6) and using the allowable limits for the elements results in a maximum PRI value of 24.3280 for all elements, which is the maximum permissible value. Consequently, the analysis is performed monthly and then compared to the established limit, as shown in Table 10. Table 10 contains the analytical results after applying the new methodological approach and shows the concentrations for various elements, including DO, TUR, BOD, TSS,

COD and oil and grease values, which categorize the level of pollution that is uncontaminated in all months. The fact that these results are consistent with those predicted by the Pollution Degree Index (PDI) shows that the methodology of this new indicator is sound. Table 11 shows the main indices published in other literature, particularly for aquatic ecosystems.

TABLE 10. Results of the PRI index

Months	Concentration						PRI	Contamination Level
	DO (mg/L)	TUR (NTU)	BOD (mg/L)	COD (mg/L)	TSS (mg/L)	OIL (mg/L)		
March	9.96	2.9433	10.15	25.8	17.91	1.13	12.2170	Uncontaminated
April	11.25	14.4516	8.42	28.6	36	1.408	9.5130	Uncontaminated
May	12.4	14.9433	13.72	33	38.4	1.932	16.6838	Uncontaminated
June	11.5	13.73	16.52	37.7	40.6	2.19	16.3283	Uncontaminated
July	10.08	15.3866	21.72	42.1	47.8	2.62	15.9639	Uncontaminated
August	9.94	15.7433	24.25	49.8	47.8	3.275	17.0535	Uncontaminated

TABLE 11. Pollution parameter indices reported in the literature, their application formula, their use in ecosystems and their field of application.

Index	Formula for application	Ecosystem	Application area	Reference
PDI	$\frac{C_s}{C_m}$	Water	The index measures water heavy metal concentrations compared to maximum allowed values.	(Ramal, Jalal, and Abdulhameed 2021)
PI	$\frac{\sqrt{[(\frac{C}{SI})_{max}^2 + (\frac{C}{SI})_{Min}^2]}}{2}$	Water	Calculations for individual metals	(Caeiro et al. 2005; Goher et al. 2014)
WQI	$\sum_{i=1}^n Q_i W_i / \sum_{i=1}^n W_i$	Water	Quantifies the combined impact of specific water quality factors on the total water quality.	(Mohammed 2013; Tyagi et al. 2020; Balan, Madan Kumar, and Shivakumar 2012)
PRI	DO (W_{DO}) + TUR (W_{TUR}) + BOD (W_{BOD}) + COD (W_{COD}) + TSS (W_{TSS}) + Oil (W_{Oil})	Water	The most proximate indicator to the index created in this study was the Water Quality Index (WQI), as it considers the elements' weights and assesses pollution based on all criteria, was the same methodology in (PRI)	The novel index of this study

PDI: pollution degree index, PI: pollution index, WQI: water quality index, PRI: physico-chemical risk index.

Figure 9 shows the degree of oil pollution in the Garraf oil field as a function of the PRI index. The results were classified based on the results of the new indicator and their

application to each sample, then the database was built in GIS and the map was created. The map was created based on the inverse distance weighting (IDW) interpolation.

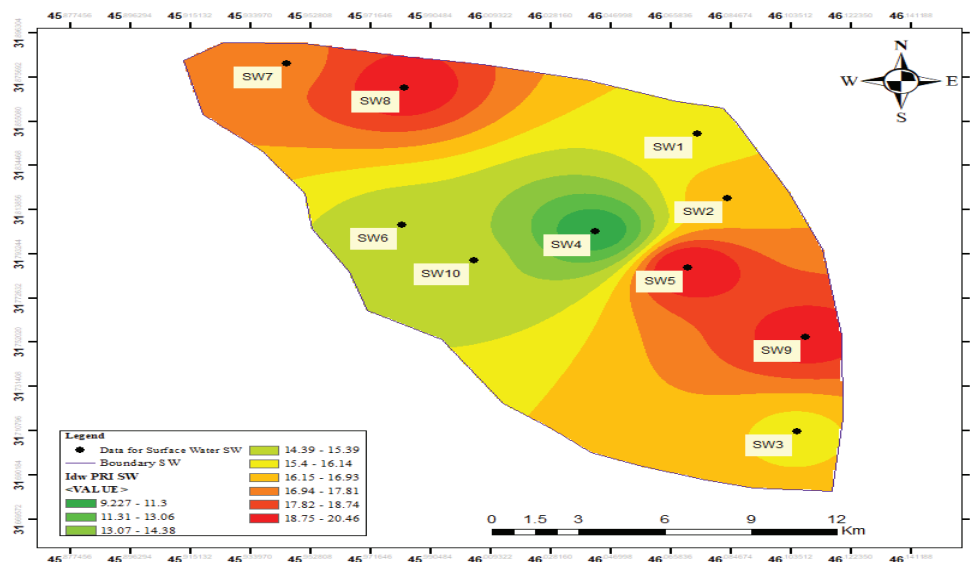


FIGURE 9. The final physico-chemical risk index (PRI) map of the Garraf Oil Field

CONCLUSION

The chemical and physical pollution maps produced show that the main potential future source of pollution in the study area is the epicenter of oil activity, particularly the regions around the oil wells in the station (SW5). These regions showed significant pollution, especially for elements such as turbidity, BOD5, COD and TSS. Compared to other indicators certified by professional organizations such as the Environmental Protection Agency (EPA) and the World Health Organization (WHO), the results of the unique technique showed that there is currently no major pollution threat.

ACKNOWLEDGEMENT

The authors would like to thank Green Engineering and Net Zero Solution (GREENZ), Universiti Kebangsaan Malaysia (UKM) for supporting this research work. The authors would also like to express their sincere gratitude to the Environmental Directorate of Thi-Qar, Iraq for their assistance in the study of the samples.

DECLARATION OF COMPETING INTEREST

None.

REFERENCES

- Abdul Maulud, Khairul Nizam, Arniza Fitri, Wan Hanna Melini Wan Mohtar, Wan Shafrina Wan Mohd Jaafar, Nur Zukrina Zuhairi, and Mohd Khairul Amri Kamarudin. 2021. A study of spatial and water quality index during dry and rainy seasons at Kelantan river basin, Peninsular Malaysia. *Arabian Journal of Geosciences* 14 (2): 85. <https://doi.org/10.1007/s12517-020-06382-8>.
- Ahmed, W., A. Vieritz, A. Goonetilleke, and T. Gardner. 2010. Health risk from the use of roof-harvested rainwater in Southeast Queensland, Australia, as potable or nonpotable water, determined using quantitative microbial risk assessment. *Applied and Environmental Microbiology* 76 (22): 7382–91. <https://doi.org/10.1128/AEM.00944-10>.
- Alssgeer, Hassan Mohammed Ali, Muhammad Barzani Gasim, Marlia M. Hanafiah, Elhadi Ramadan Ali Abdulhadi, and Azman Azid. 2018. GIS-based analysis of water quality deterioration in the Nerus River, Kuala Terengganu, Malaysia. *Desalination and Water Treatment* 112 (June): 334–43. <https://doi.org/10.5004/dwt.2018.22335>.

- Anjum, Mavia. n.d. Quality evaluation and health implications of natural spring water from a district in outer himalayas : A case study for Murree , Pakistan.
- Arslan, I. 2001. Treatability of a simulated disperse dye-bath by ferrous iron coagulation, ozonation, and ferrous iron-catalyzed ozonation. *Journal of Hazardous Materials* 85 (3): 229–41. [https://doi.org/10.1016/S0304-3894\(01\)00232-1](https://doi.org/10.1016/S0304-3894(01)00232-1).
- Ashkanani, Amal, F. Almomani, Majeda Khraishah, R. Bhosale, Muhammad Tawalbeh, and Khaled AlJaml. 2019. Bio-carrier and operating temperature effect on ammonia removal from secondary wastewater effluents using Moving Bed Biofilm Reactor (MBBR). *Science of the Total Environment* 693: 133425. <https://doi.org/10.1016/j.scitotenv.2019.07.231>.
- Ata, Frankie Marcus, Mohd Khairul Amri Kamarudin, Nadzifah Yaakub, Noorjima Abd. Wahab, Mohd Ekhwani Toriman, Hafizan Juahir, Muhammad Barzani Gasim, et al. 2018. Impact of hydrological study to water quality status in Kuantan River, Pahang, Malaysia. *International Journal of Engineering and Technology(UAE)* 7 (3.14 Special Issue 14): 35–43. <https://doi.org/10.14419/ijet.v7i3.14.16859>.
- Balan, INanda, PD Madan Kumar, and M Shivakumar. 2012. An assessment of groundwater quality using water quality index in Chennai, Tamil Nadu, India. *Chronicles of Young Scientists* 3 (2): 146. <https://doi.org/10.4103/2229-5186.98688>.
- Bilotta, G. S., and R. E. Brazier. 2008. Understanding the influence of suspended solids on water quality and aquatic biota. *Water Research* 42 (12): 2849–61. <https://doi.org/10.1016/j.watres.2008.03.018>.
- Bukhari, Alaadin A. 2008. Investigation of the electro-coagulation treatment process for the removal of total suspended solids and turbidity from municipal wastewater. *Bioresource Technology* 99 (5): 914–21. <https://doi.org/10.1016/j.biortech.2007.03.015>.
- Caeiro, S., M.H. Costa, T.B. Ramos, F. Fernandes, N. Silveira, A. Coimbra, G. Medeiros, and M. Painho. 2005. Assessing heavy metal contamination in sado estuary sediment: An index analysis approach. *Ecological Indicators* 5 (2): 151–69. <https://doi.org/10.1016/j.ecolind.2005.02.001>.
- Chen, Kai, Qimeng Liu, Tingting Yang, Qiding Ju, and Mingfei Zhu. 2024. Risk assessment of nitrate groundwater contamination using GIS-based machine learning methods: A case study in the Northern Anhui Plain, China. *Journal of Contaminant Hydrology* 261 (February): 104300. <https://doi.org/10.1016/j.jconhyd.2024.104300>.
- Das, Panchanan. 2019. *Econometrics in Theory and Practice: Analysis of Cross Section, Time Series and Panel Data with Stata 15.1*. *Econometrics in Theory and Practice: Analysis of Cross Section, Time Series and Panel Data with Stata 15.1*. <https://doi.org/10.1007/978-981-32-9019-8>.
- Dheenana, P. S., Dilip Kumar Jha, N. V. Vinithkumar, A. Angelin Ponmalar, P. Venkateshwaran, and R. Kirubakaran. 2014. Spatial variation of physicochemical and bacteriological parameters elucidation with GIS in Rangat Bay, Middle Andaman, India. *Journal of Sea Research* 85: 534–41. <https://doi.org/10.1016/j.seares.2013.09.001>.
- Dongquan, Zhao, Chen Jining, Wang Haozheng, Tong Qingyuan, Cao Shangbing, and Sheng Zheng. 2009. GIS-based urban rainfall-runoff modeling using an automatic catchment-discretization approach: A case study in Macau. *Environmental Earth Sciences* 59 (2): 465–72. <https://doi.org/10.1007/s12665-009-0045-1>.
- El-Zeiny, Ahmed M., and Salwa F. Elbeih. 2019. GIS-based evaluation of groundwater quality and suitability in Dakhla Oases, Egypt. *Earth Systems and Environment* 3 (3): 507–23. <https://doi.org/10.1007/s41748-019-00112-1>.
- Falih, K. T., S. F. Mohd Razali, K. N. Abdul Maulud, N. Abd Rahman, S. I. Abba, and Z. M. Yaseen. 2024. Assessment of petroleum contamination in soil, water, and atmosphere: A comprehensive review. *International Journal of Environmental Science and Technology*, April. <https://doi.org/10.1007/s13762-024-05622-8>.
- Frutos, F. Javier García, Olga Escolano, Susana García, Mar Babín, and M. Dolores Fernández. 2010. Bioventing remediation and ecotoxicity evaluation of phenanthrene-contaminated soil. *Journal of Hazardous Materials*. <https://doi.org/10.1016/j.jhazmat.2010.07.098>.
- Gandaseca, Seca, Noraini Rosli, Johin Ngayop, and Chandra Iman Arianto. 2011. Status of water quality based on the physico-chemical assessment on river water at Wildlife Sanctuary Sibuti Mangrove Forest, Miri Sarawak. *American Journal of Environmental Sciences* 7 (3): 269–75. <https://doi.org/10.3844/ajessp.2011.269.275>.
- Goher, Mohamed E., Ali M. Hassan, Ibrahim A. Abdel-Moniem, Ayman H. Fahmy, and Seliem M. El-Sayed. 2014. Evaluation of surface water quality and heavy metal indices of Ismailia Canal, Nile River, Egypt. *Egyptian Journal of Aquatic Research* 40 (3): 225–33. <https://doi.org/10.1016/j.ejar.2014.09.001>.
- Gong, Gordon, Sravan Mattevada, and Sid E. O'Bryant. 2014. Comparison of the accuracy of kriging and idw interpolations in estimating groundwater arsenic concentrations in Texas. *Environmental Research* 130: 59–69. <https://doi.org/10.1016/j.envres.2013.12.005>.
- Haldar, Kamonashish, Katarzyna Kujawa-Roeleveld, Priyanka Dey, Shanchita Bosu, Dilip Kumar Datta, and Huub H.M. Rijnaarts. 2020. Spatio-temporal variations in chemical-physical water quality parameters influencing water reuse for irrigated agriculture in tropical urbanized deltas. *Science*

- of the *Total Environment* 708: 134559. <https://doi.org/10.1016/j.scitotenv.2019.134559>.
- Ikechukwu, Maduako Nnamdi, Elijah Ebinne, Ufot Idorenyin, and Ndukwu Ike Raphael. 2017. Accuracy assessment and comparative analysis of IDW, spline and kriging in spatial interpolation of landform (topography): An experimental study. *Journal of Geographic Information System* 09 (03): 354–71. <https://doi.org/10.4236/jgis.2017.93022>.
- Jones, Norman L, R. Jeffrey Davis, and Walid Sabbah. 2003. A comparison of three-dimensional interpolation techniques for plume characterization. *Ground Water* 41 (4): 411–19. <https://doi.org/10.1111/j.1745-6584.2003.tb02375.x>.
- Jurgelenaite, Aldona, Jurate Kriauciuniene, and Diana Šarauskiene. 2012. Spatial and temporal variation in the water temperature of Lithuanian Rivers. *Baltica* 25 (1): 65–76. <https://doi.org/10.5200/baltica.2012.25.06>.
- Khan, Mohd Yawar Ali, Khalid Muzamil Gani, and Govind Joseph Chakrapani. 2016. Assessment of surface water quality and its spatial variation. A case study of Ramganga River, Ganga Basin, India. *Arabian Journal of Geosciences* 9 (1): 1–9. <https://doi.org/10.1007/s12517-015-2134-7>.
- Khouni, Imen, Ghofrane Louhichi, and Ahmed Ghrabi. 2021. Use of GIS based inverse distance weighted interpolation to assess surface water quality: Case of Wadi El Bey, Tunisia. *Environmental Technology and Innovation* 24: 101892. <https://doi.org/10.1016/j.eti.2021.101892>.
- Li, Jin, and Andrew D. Heap. 2011. A review of comparative studies of spatial interpolation methods in environmental sciences: Performance and impact factors. *Ecological Informatics* 6 (3–4): 228–41. <https://doi.org/10.1016/j.ecoinf.2010.12.003>.
- Mhamdi, Fodha, Imen Khouni, and Ahmed Ghrabi. 2016. Diagnosis and characteristics of water quality along the Wadi El Bey River (Tunisia). Coagulation/flocculation essays of textile effluents discharged into the Wadi. *Desalination and Water Treatment* 57 (46): 22166–88. <https://doi.org/10.1080/19443994.2016.1147378>.
- Mirzaei, Rouhollah, and Mohamad Sakizadeh. 2016. Comparison of interpolation methods for the estimation of groundwater contamination in Andimeshk-Shush Plain, Southwest of Iran. *Environmental Science and Pollution Research* 23 (3): 2758–69. <https://doi.org/10.1007/s11356-015-5507-2>.
- Mohamad Hamzah, Firdaus, Mohd Nabil Fikri, Izamarlina Asshaari, Mohd Saifullah Rusiman, Mohd Khairul Amri Kamarudin, and Shamsul Rijal Muhammad Sabri. 2022. Spatial and temporal assessment of marine water quality using statistical approaches. *Jurnal Kejuruteraan* si5 (2): 23–34. [https://doi.org/10.17576/jkukm-2022-si5\(2\)-03](https://doi.org/10.17576/jkukm-2022-si5(2)-03).
- Mohammed, Fadhil Mohamed Al-. 2013. Application of water quality index for evaluation of groundwater quality for drinking purpose in Dibdiba Aquifer, Kerbala City, Iraq. *Journal of Babylon University/Engineering Sciences* 21 (5): 1647–1660.
- Mohd Soukhri, Danial Nakhaie, Siti Multazimah Mohamad Faudzi, Zuriyati Yusof, Mohd Fitri Mohd Akhir, Nurzulaikha Mohd Kamal, and Noor Aida Saad. 2022. A review on factors to be incorporated in water quality study. *Jurnal Kejuruteraan* 34 (4): 575–83. [https://doi.org/10.17576/jkukm-2022-34\(4\)-05](https://doi.org/10.17576/jkukm-2022-34(4)-05).
- Mtewa, S., S. Kusangaya, and C. F. Schutte. 2003. The application of Geographic Information Systems (GIS) in the analysis of nutrient loadings from an agro-rural catchment. *Water SA* 29 (2): 189–93. <https://doi.org/10.4314/wsa.v29i2.4855>.
- Muhammad, Said, and Qazi Ahmed Usman. 2022. Heavy Metal Contamination in Water of Indus River and Its Tributaries, Northern Pakistan: Evaluation for Potential Risk and Source Apportionment. *Toxin Reviews* 41 (2): 380–88. <https://doi.org/10.1080/15569543.2021.1882499>.
- Nguyen, Giao Thanh, Mi Le Thi Diem, and Nhien Thi Hong Huynh. 2023. Pollution and Risk Level Assessment of Pollutants in Surface Water Bodies. *Civil Engineering Journal (Iran)* 9 (8): 1851–62. <https://doi.org/10.28991/CEJ-2023-09-08-03>.
- Nguyen, Giao Thanh, and Dan Hoang Truong. 2023. Risks of Surface Water Pollution in Southern Vietnam. *Civil Engineering Journal (Iran)* 9 (11): 2725–35. <https://doi.org/10.28991/CEJ-2023-09-11-06>.
- Njeban, Hassan Swadi. 2018. Comparison and Evaluation of GIS-Based Spatial Interpolation Methods for Estimation Groundwater Level in AL-Salman District—Southwest Iraq. *Journal of Geographic Information System* 10 (04): 362–80. <https://doi.org/10.4236/jgis.2018.104019>.
- Noraini Ruslan, Jannatulhawa Jasni, Nurul Fatini Yusri. 2021. Assessment of water quality and heavy metals in drainage canal. *International Research Journal of Modernization in Engineering Technology and Science* 3 (9).
- Oke, Adebayo Olubukola, and Kolawole Ogedengbe. 2013. Mapping of River Water Quality Using Inverse Ogun-Osun River Basin, Nigeria. *Lanskap & Environment* 7 (2): 48–62.
- Okonofua, Ehizonomhen Solomon, Kayode Hassan Lasisi, and Sunday Egbiki. 2020. Modeling the Reaction and Transport Mechanism for Total Petroleum Hydrocarbon Using Selected Linear and Nonlinear Error Functions. *Jurnal Kejuruteraan* 32 (4): 621–27. [https://doi.org/10.17576/jkukm-2020-32\(4\)-09](https://doi.org/10.17576/jkukm-2020-32(4)-09).
- Panigrahy, Supriya. 2021. Geospatial Crime Analytics: A GIS-Based Approach Towards Prediction of Crime Hotspots. *Journal of LATEX Templates*. <https://engrxiv.org/preprint/view/1654>.

- Pankalakar, S. S., and A. P. Jarag. 2016. Assessment of Spatial Interpolation Techniques for River Bathymetry Generation of Panchganga River Basin Using Geoinformatic Techniques. *Asian Journal of Geoinformatics* 15 (3): 9–15. <http://203.159.29.7/index.php/journal/article/view/240>.
- Proshad, Ram, Saiful Islam, Tanmoy Roy Tusher, Dan Zhang, Sujana Khadka, Jianing Gao, and Satyajit Kundu. 2021. Appraisal of Heavy Metal Toxicity in Surface Water with Human Health Risk by a Novel Approach: A Study on an Urban River in Vicinity to Industrial Areas of Bangladesh. *Toxin Reviews* 40 (4): 803–19. <https://doi.org/10.1080/15569543.2020.1780615>.
- Putnam, By James E, and Larry M Pope. 2003. Trends in Suspended-sediment concentration at selected stream sites in Kansas , 1970 – 2002. *Sites The Journal Of 20Th Century Contemporary French Studies*.
- Qiao, Pengwei, Mei Lei, Sucai Yang, Jun Yang, Guanghui Guo, and Xiaoyong Zhou. 2018. Comparing ordinary kriging and inverse distance weighting for soil as pollution in Beijing. *Environmental Science and Pollution Research* 25 (16): 15597–608. <https://doi.org/10.1007/s11356-018-1552-y>.
- Ramal, Majeed Mattar, Arkan Dhari Jalal, and Uday Hatem Abdulhameed. 2021. Heavy metal assessment in taps drinking water of ramadi city using water quality indices, Anbar Province, Iraq. *International Journal of Sustainable Development and Planning* 16 (7): 1349–57. <https://doi.org/10.18280/ijmdp.160715>.
- Reza, R., and G. Singh. 2010. Heavy metal contamination and its indexing approach for river water. *International Journal of Environmental Science and Technology* 7 (4): 785–92. <https://doi.org/10.1007/BF03326187>.
- Schweitzer, Linda, and James Noblet. 2018. Water contamination and pollution. In *Green Chemistry: An Inclusive Approach*, 261–90. Elsevier Inc. <https://doi.org/10.1016/B978-0-12-809270-5.00011-X>.
- Sekulić, Aleksandar, Milan Kilibarda, Gerard B.M. Heuvelink, Mladen Nikolić, and Branislav Bajat. 2020. Random forest spatial interpolation. *Remote Sensing* 12 (10): 1–29. <https://doi.org/10.3390/rs12101687>.
- Simpson, Greg, and Yi Hwa Wu. 2014. Accuracy and effort of interpolation and sampling: Can GIS help lower field costs? *ISPRS International Journal of Geo-Information* 3 (4): 1317–33. <https://doi.org/10.3390/ijgi3041317>.
- Singh, Rupanjali, C.B. Majumder, and Ajit Kumar Vidyarthi. 2023. Assessing the impacts of industrial wastewater on the inland surface water quality: An application of Analytic Hierarchy Process (AHP) model-based water quality index and GIS techniques. *Physics and Chemistry of the Earth, Parts A/B/C* 129 (February): 103314. <https://doi.org/10.1016/j.pce.2022.103314>.
- Syed Abdul Rahman, Syed Ahmad Fadhli, Khairul Nizam Abdul Maulud, Sharifah Nurul Ain Syed Mustorpha, Sarah Shaharuddin, and Adi Irfan Che Ani. 2022. Implementation of BIM-GIS geometry for user navigation in the indoor environment: A review. *Jurnal Kejuruteraan* 34 (2): 211–21. [https://doi.org/10.17576/jkukm-2022-34\(2\)-04](https://doi.org/10.17576/jkukm-2022-34(2)-04).
- Tyagi, SWater Quality Assessment in Terms of Water Quality Indexhweta, Bhavtosh Sharma, Prashant Singh, and Rajendra Dobhal. 2020. Water quality assessment in terms of water quality index. *American Journal of Water Resources* 1 (3): 34–38. <https://doi.org/10.12691/ajwr-1-3-3>.
- U.Farooq, M., Muhammad Waseem, Sadia Mazhar, Anjum Khairi, and Talha Kamal. 2015. A review on Internet of Things (IoT). *International Journal of Computer Applications* 113 (1): 1–7. <https://doi.org/10.5120/19787-1571>.
- Wan Mohtar, Wan Hanna Melini, Khairul Nizam Abdul Maulud, Nur Shazwani Muhammad, Suraya Sharil, and Zaher Mundher Yaseen. 2019. Spatial and temporal risk quotient based river assessment for water resources management. *Environmental Pollution* 248 (May): 133–44. <https://doi.org/10.1016/j.envpol.2019.02.011>.
- Wilk, Julie, Dominic Kniveton, Lotta Andersson, Russell Layberry, Martin C. Todd, Denis Hughes, Susan Ringrose, and Cornelis Vanderpost. 2006. Estimating rainfall and water balance over the Okavango River basin for hydrological applications. *Journal of Hydrology* 331 (1–2): 18–29. <https://doi.org/10.1016/j.jhydrol.2006.04.049>.
- Wu, Chia Yu, Joann Mossa, Liang Mao, and Mohammad Almulla. 2019. Comparison of different spatial interpolation methods for historical hydrographic data of the lowermost Mississippi River. *Annals of GIS* 25 (2): 133–51. <https://doi.org/10.1080/19475683.2019.1588781>.
- Yavuz, Hüseyin, and Saffet Erdoğan. 2012. Spatial analysis of monthly and annual precipitation trends in Turkey. *Water Resources Management* 26 (3): 609–21. <https://doi.org/10.1007/s11269-011-9935-6>.
- Zaiedy, Norshahkilla Izzatul, Othman A. Karim, and Nurul Afina Abd Mutalib. 2016. Water quality of surface runoff in loop two catchment area in UKM. *Jurnal Kejuruteraan* 28 (1): 65–72. <https://doi.org/10.17576/jkukm-2016-28-07>.